BIOCHEMISTRY
including biophysical chemistry & molecular biology

Article

pubs.acs.org/biochemistry

Ion Binding and Internal Hydration in the Multidrug Resistance Secondary Active Transporter NorM Investigated by Molecular Dynamics Simulations

Stefano Vanni,[†] Pablo Campomanes,[†] Marco Marcia,[‡] and Ursula Rothlisberger*[,†]

[†]Laboratory of Computational Chemistry and Biochemistry, Ecole Polytechnique Fédérale Lausanne, CH-1015 Lausanne, Switzerland

[‡]Department of Molecular, Cellular and Developmental Biology, Yale University, New Haven, Connecticut 06511, United States

Supporting Information

ABSTRACT: Recently, a 3.65 Å resolution structure of the transporter NorM from the multidrug and toxic compound extrusion family has been determined in the outward-facing conformation. This antiporter uses electrochemical gradients to drive substrate export of a large class of antibiotic and toxic compounds in exchange for small monovalent cations (H^+ and Na^+), but the molecular details of this mechanism are still largely unknown. Here we report all-atom molecular dynamics simulations of NorM, with and without the bound Na^+ cation and at different ion concentrations. Spontaneous binding of Na^+ is observed in several independent simulations with transient ion binding to D36 being necessary to reach the final binding site for which two competitive binding modes occur. Finally, the simulations indicate that the extracellular vestibule of the transporter invariably loses its characteristic V shape indicated by the crystallographic data, and it is reduced to a narrow permeation pathway lined by polar residues that can act as a specific pore for the transport of small cations. This event, together with the available structures of evolutionarily related transporters of the major facilitator superfamily (MFS), suggests that differences in the hydrophobic content of the extracellular vestibule may be characteristic of multidrug resistance transporters in contrast to substrate-selective members of the MFS.

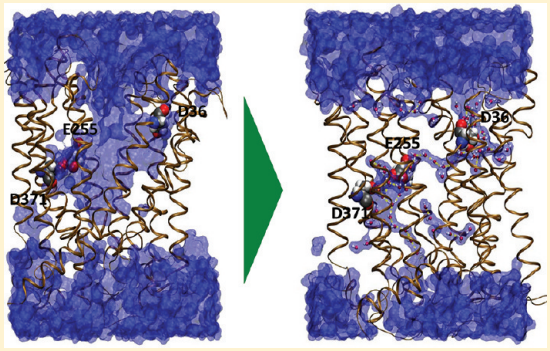

The ability of infectious microorganisms and tumors to acquire multidrug resistance (MDR) is a crucial factor in their pathogenicity. A key role in this process is played by multidrug efflux transporters, integral membrane proteins that mediate the export of various compounds to the outside of the cell via either primary or secondary active transport. In recent years, crystal structures have been determined for a number of multidrug transporters,[1−4] providing evidence at the molecular level of a general mechanism proposed several years ago for drug extrusion, the alternating-access model.[5] In this framework, the catalytic cycle of the transporter involves sequential conformational changes of the carrier protein with only limited movement of the substrate binding site. Alternate accessibility of this site from one side of the membrane or the other gives rise to two main conformations, named outward-facing and inward-facing, which cyclically alternate, leading to substrate transport driven by the transmembrane electrochemical potential.[5−8]

Recently, the three-dimensional structure of NorM, a member of the new multidrug and toxic compound extrusion (MATE) family of transporters, has been determined by X-ray crystallography in its outward-facing conformation.[9] MATE transporters use either H^+ or Na^+ gradients across the membrane to drive substrate export, and they are responsible for the extrusion of a large class of antibiotic and toxic compounds.[10] Interestingly, the topology of NorM, which consists of two bundles of six transmembrane (TM) helices, differs from those of the other known 12-TM transporters,[9,11] because the four three-helix bundles that compose the transporter are not intersected by any transmembrane helix that belongs to a different bundle. Therefore, this protein represents an interesting system for improving our understanding of the mechanistic details of the alternating-access model, especially in comparison with what has recently been proposed for the transporters of the major facilitator superfamily (MFS),[12,13] and for investigating the origin of the wide polyspecificity of MDR transporters in contrast with the narrow specificity of non-MDR transporters of the MFS.[14−16]

Despite the medium resolution (3.7 Å), the crystal structure revealed interesting features, but it also raised a number of questions. First, the coordination of the rubidium cation (that occupies a putative Na^+ binding site) with the two residues that have been shown to be crucial in the transport activity of NorM,[17] E255 and D371, is not obvious, while it appears that

Received: September 30, 2011
Revised: January 9, 2012
Published: January 17, 2012

several aromatic residues (F259, F288, F429, Y367, and Y395) are located closer the electron density attributed to the ion.

Second, D36, a residue that has been shown to be crucial for transport activity by mutagenesis experiments,[17] is not in obvious structural proximity to the pathway through which the monovalent cation can access the binding pocket. Consequently, it remains unclear how this residue takes part in the mechanism of ion transport in NorM.

Moreover, the crystallographic data reveal only one of the many conformational states that NorM is expected to sample during the whole transport cycle, according to the alternating-access model. For instance, on the basis of the currently available NorM structures, it is impossible to describe how cation binding triggers NorM to assume its inward-facing conformation.

These observations suggest that a stand-alone analysis of the crystallographic structure is not sufficient to clarify important aspects of the mechanism of drug extrusion by this secondary active antiporter, and that information about the dynamical behavior of the transporter would be of fundamental medical and pharmaceutical importance for tackling the serious problem of multidrug resistance.

To address these questions, we performed nine independent all-atom molecular dynamics (MD) simulations of NorM in a lipid bilayer, with and without bound cation and at different ion concentrations for a cumulative length of 2.3 μs. Our results shed light on the molecular basis of the mechanism of drug extrusion in the MATE family, providing an atomic-level description of how sodium binds to the outward-facing conformation of the transporter and how this binding event triggers conformational changes in the cytoplasmic face of the transporter. In addition, our simulations indicate how differences in the hydrophobic content of the extracellular vestibule may characterize multidrug resistance transporters (NorM and EmrD) in contrast to more substrate-selective members of the MFS (FucP, LacY, and GlpT).

MATERIALS AND METHODS

All simulations are based on the crystal structure of *Vibrio cholerae* NorM [Protein Data Bank (PDB) entry 3MKT],[9] either in its apo form or bound to a sodium ion that was inserted into the protein at the same position as the rubidium electron density found in the other structure of NorM (PDB entry 3MKU).[9] All ionizable side chains, including D36, E255, and D371, as well as the C- and N-termini were modeled in their default ionization state. The protein was inserted in a pre-equilibrated palmitoyloleoylphosphatidylethanolamine (POPE) membrane using g_membed,[18] and all data collections and equilibration runs were performed using GROMACS 4.[19] The system was immersed in a box of water with dimensions of ~86 Å × ~86 Å × ~93 Å containing 12600 molecules. The box dimensions are chosen in such a way that the minimal distance between periodic images of the protein is always >30 Å during the simulation. The total number of atoms in our models is ~70000. After insertion of the protein, the system was minimized using a steepest descent algorithm and then heated to 310 K over 620 ps while positional restraints were maintained on crystallographic C_α atoms (C_αs) that were slowly removed in two successive runs of 4 ns at 310 K. Positional restraints on crystallographic C_αs were set to 1000 and 100 kJ mol^{-1} nm^{-2}.

The all-atom CHARMM36[20,21] force field was used in combination with the TIP3P[22] model for water; electrostatic interactions were calculated with the Ewald particle mesh method,[23] with a real space cutoff of 12 Å. Bonds involving hydrogen atoms were constrained using the LINCS[24] algorithm, and the integration time step was set to 2 fs. The system was coupled to a Bussi thermostat[25] and to a semi-isotropic Berendsen barostat[26] at a temperature of 310 K and a pressure of 1 atm.

All data analysis were conducted using GROMACS[19] utilities, and all molecular images were made with Visual Molecular Dynamics (VMD),[27] with the exception of Figures S1 and S2 of the Supporting Information that were made using PyMol.[28] Details concerning the length and ion concentration of the different simulations are listed in Table 1. The four simulations with 10 Na^+ ions to study entry of Na^+ into the transporter have been started after 10 ns (two runs) and after 100 ns (two runs) of the two simulations without Na^+ ions. Root-mean-square deviation (rmsd) and root-mean-square fluctuation (rmsf) analyses can be found in Figures S3−S7 of the Supporting Information.

Table 1. Details of the Nine Independent MD Simulations of NorM[a]

MD simulation	initial binding state	total no. of Na^+ atoms	simulation length (ns)	first binding to D36 (ns)	first binding to E255/D371 (ns)
a	bound	1	280	na	na
b	bound	1	320	na	na
c	bound	23	310	–	–
d	empty	0	200	na	na
e	empty	0	200	na	na
f	empty	10	40	9	11
g	empty	10	465	243	–
h	empty	10	295	241	–
i	empty	10	220	–	–

[a]In MD runs a and b, no spontaneous binding to D36 or E255/D371 can take place because the only Na^+ ion present in the system is already bound to E255/D371. In MD run c, no spontaneous binding to D36 or E255/D371 is observed while a Na^+ is already present in the binding pocket. In MD runs d and e, spontaneous binding cannot be observed because no Na^+ ions are present in the bulk.

RESULTS AND DISCUSSION

The Extracellular Vestibule of NorM Loses Its V Shape in the MD Simulations, Being Reduced to a Narrow Permeation Pathway. The crystal structure of NorM has been determined in the outward-facing conformation. It presents a large extracellular vestibule that allows the permeation of water from the extracellular medium (Figure 1a−c). Figure 1c shows the water content of NorM in MD simulations where the C_αs of the protein are restrained to the crystallographic positions. Because of the presence of a large extracellular lumen, the internal cavity of the protein becomes immediately entirely solvated within a few nanoseconds during equilibration.

To study the conformational stability of the outward-facing conformation of NorM, we started five MD simulations from the crystallographic structure. In two of them (MD runs a and b), a sodium ion is inserted into the protein in the position of the rubidium electron density. In a third simulation (MD run c), no sodium ion is inserted into the protein but the system is simulated at a physiological ion concentration. Immediately during equilibration, while the C_αs of the protein are restrained

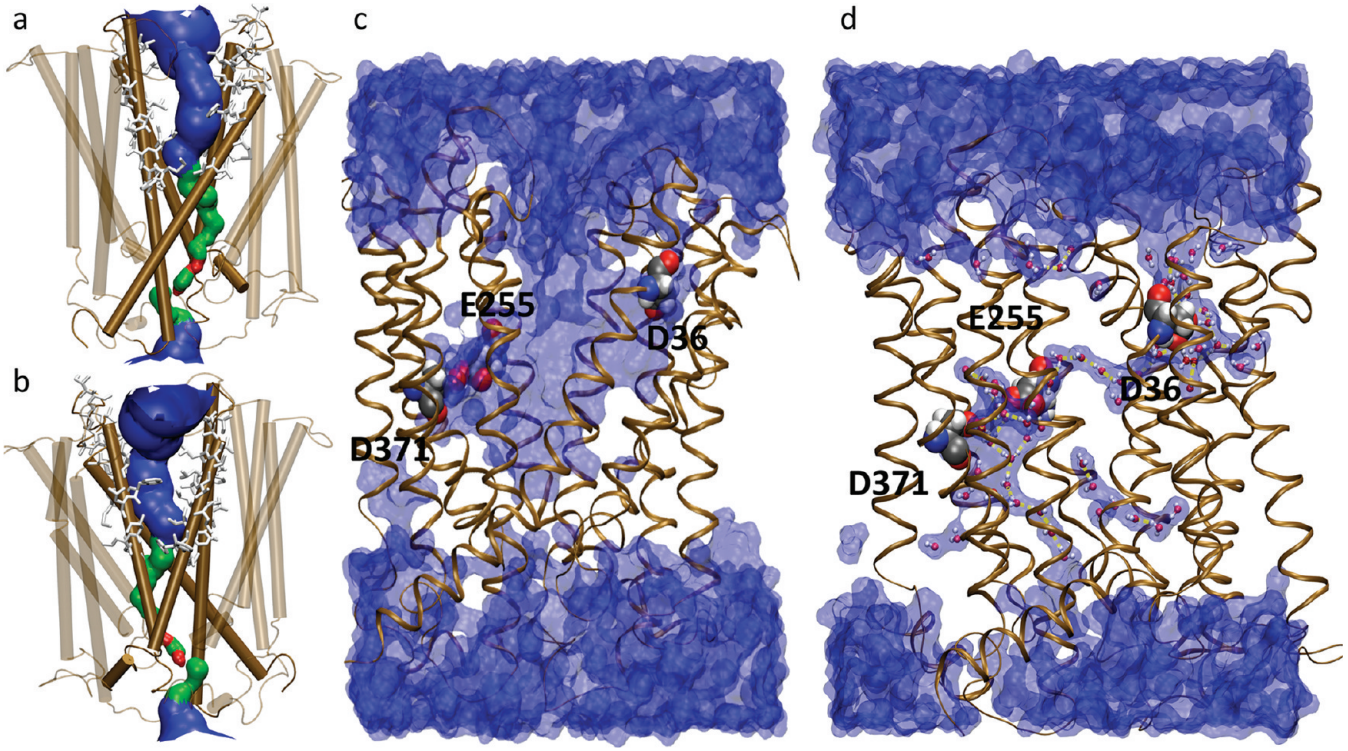

Figure 1. (a) Front and (b) rear views of the central cavity in the crystal structure of NorM computed using HOLE.[34] The color code is indicative of the radius of the pore, with parts that are inaccessible to water (pore radius of <1.15 Å) colored red, water accessible parts (pore radius between 1.15 and 2.30 Å) colored green, and wide areas (pore radius of >2.30 Å) colored blue. Helices 1 and 2 and helices 7 and 8, constituting the transmembrane bundle that forms the extracellular vestibule, are depicted in ochre, while all other helices are colored transparently. All hydrophobic residues (Val, Ala, Leu, Met, Iso, Phe, and Trp) belonging to the extracellular moiety of these four helices are depicted as white licorice. (c and d) Water accessibility (blue) in the crystal structure of NorM resulting from MD simulations of the transporter with restrained C_αs (c) and representative structure of the transporter in several independent unconstrained MD simulations (d). The latter suggests that a tight pathway connects the external environment with the catalytic site, while the crystallographic structure indicates the presence of a large unselective funnel. Functionally important residues D36, E255, and D371[17] are shown in van der Waals representation. Water molecules present in the collapsed conformation of the vestibule of the transporter are explicitly shown as balls and sticks, and hydrogen bonds connecting them are colored yellow.

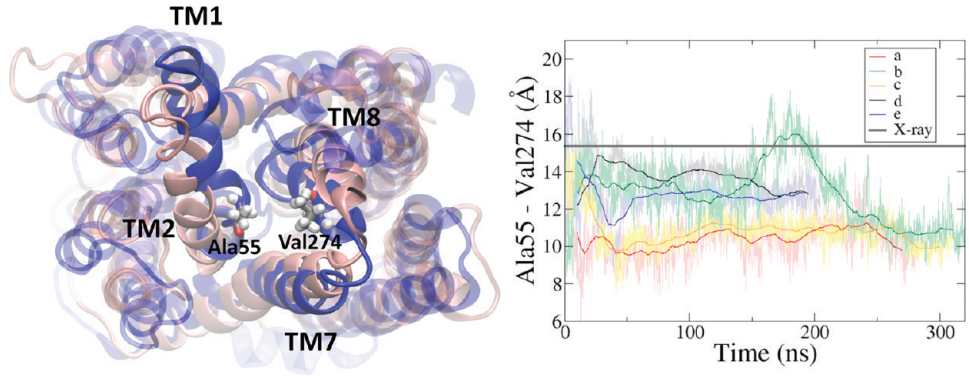

Figure 2. Extracellular vestibule collapse in the MD simulation. The left panel shows an extracellular view of the NorM lumen in the crystal structure (pink) and in one representative MD simulation (blue). TM1−2 and TM7−8, the helices that form the vestibule, are explicitly represented, while the other helices are colored transparently. Residues A55 and V274, located in TM2 and TM8, respectively, are explicity shown as licorice. The right panel shows the time evolution of the distance between the C_αs of residues A55 and V274 in independent MD simulations (see Table 1). In MD runs a−c, a sodium ion is bound to the binding pocket suggested by the crystallographic structure, while in MD runs d and e, the transporter is without a bound cation. In all simulations, the distance between the two residues, which belong to TM2 and TM8, is substantially reduced with respect to the crystallographic one (indicated with a gray bar).

to the crystallographic positions, a sodium ion enters the cavity and positions itself in the binding pocket suggested by the X-ray structure. In light of this event, we will consider MD run c as a fully bound MD run. Finally, two simulations (MD runs d and e) have been started from the apo form of the transporter. To prevent any spontaneous binding event during equilibration, these simulations have been started with no Na^+ ions, but only Cl^- ions are present to neutralize the overall system.

Once all positional restraints on crystallographic C_αs were removed, both in the apo form and in the simulations where a Na^+ is bound to the transporter in the binding site suggested by the X-ray data, the extracellular vestibule invariably loses its V

dx.doi.org/10.1021/bi2015184 | *Biochemistry* 2012, 51, 1281−1287

shape within tens of nanoseconds in all five simulations (MD runs a−e), and the large funnel that is suggested by the crystal structure is always reduced, within hundreds of nanoseconds, to a narrow and twisting water wire that connects all the charged residues that are located in the transmembrane region of the transporter (Figure 1d and Figure S8 of the Supporting Information). This transition takes place through a relative motion of TM1−2 toward TM7−8, leading to a partial closure of the large water funnel (Figure 2, left panel) that allows the system to reach an equilibrium conformation that is substantially different (average rmsd of 4 Å) from that suggested by the crystal structure.

To quantify the extent of this structural change, we monitored the distance between residues Ala55 and Val274, belonging to helices TM2 and TM8, respectively, that are located at the gates of the extracellular cavity (Figure 2, right panel). In all simulations, the distance between these two residues is substantially reduced with respect to the crystal structure (by 3−5 Å), indicating a narrowing of the extracellular lumen. Interestingly, the residues in the loop between TM1 and TM2 and those at the N-terminal end of TM2 (residues 43−54) are characterized by *B* factors of ∼160 Å^2, well above the average *B* factor of the overall structure (133 Å^2), and they correspond to one of the regions with the highest *B* factors in the structure [only the loop between TM3 and TM4 has higher *B* factors (see Table S1 of the Supporting Information)], thus suggesting conformational flexibility in the outward-facing cavity.

In addition, we investigated whether the V shape of the extracellular vestibule of NorM could originate with crystal packing contacts (Figure S1 of the Supporting Information). The two monomers forming the asymmetric unit in the crystal are oriented back to back and come in contact with each other through the surface of NorM that would face the cytoplasm in vivo (loop 2 and loop 8). The contacts with molecules belonging to other asymmetric units are instead of two types. One involves two loop 5 regions (connecting TM5 and TM6) in neighboring chains, while the second involves loop 11 (connecting TM11 and TM12) in one chain and loop 9 (connecting TM9 and TM10) in a neighboring molecule. None of these three interactions actively holds TM2 to prevent it from collapsing, as we observe in the simulations. Additionally, there is also no crystal packing constraint that induces the outward-facing surface of the protein to form an open cavity.

A closer inspection of the amino acid sequence in this region could indicate why the collapse observed in the MD simulations is taking place: the structural deformation is triggered by the fact that several hydrophobic residues in the outer part of helices 1 and 2 and helices 7 and 8 point toward the inner cavity in the crystal structure (Figure 1a,b), giving rise to unfavorable interactions with the water molecules of the external environment. As a consequence, direct contacts between hydrophobic residues present in the extracellular cavity form within nanoseconds while dewetting of the lumen takes place (Figure S8 of the Supporting Information).

The hydrophobic character of the extracellular vestibule of NorM is in contrast with most of the other determined transporter structures of the evolutionarily related MFS (GlpT,[29] LacY,[15] and FucP[12]) that show a largely hydrophilic vestibule, the only exception being the multidrug antiporter EmrD[3] (Figure 3). Like NorM, this transporter has a largely hydrophobic central cavity, and most notably, it does not present a V shape in the crystal structure.[3] While the

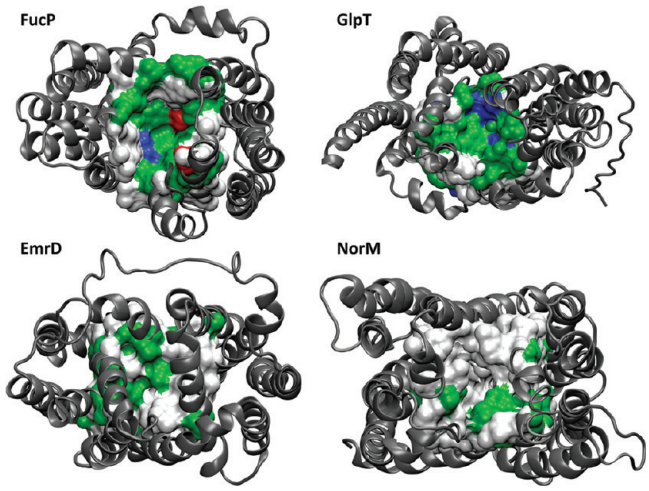

Figure 3. Hydrophobic content of the vestibule of NorM and of other MFS transporters. Top view of the crystal structures of FucP,[12] GlpT,[29] EmrD,[3] and NorM.[9] The internal cavity of the transporter is depicted in surface representation with the following color code: white for hydrophobic residues, green for polar residues, red for negatively charged residues, and blue for positively charged residues. Transporters involved in multidrug resistance (EmrD and NorM) show an increased hydrophobic content with respect to non-MDR ones (FucP and GlpT). The difference in hydrophobic content could also explain the lower stability of the V-shaped conformation for the MDR transporters as suggested by X-ray crystallography (EmrD[3]) and molecular dynamics simulations (NorM).

hydrophilic character of the vestibule of GlpT, LacY, and FucP is probably necessary to achieve the high specificity of these transporters for a given substrate, the extensive hydrophobic character of the vestibule of EmrD and NorM might be related to their similar role as MDR antiporters able to extrude a large variety of hydrophobic molecules. This remarkable difference in hydrophobic content might also give a possible rationale for the observed occluded conformation of EmrD in the X-ray structure and for the collapse of the V shape of NorM in the MD simulations. It is indeed possible that during the catalytic cycle of the transporter, the V-shaped conformation is only a short-lived intermediate in the absence of the transported substrate. In fact, unlike other transporters, the extracellular vestibule of NorM does not have to bind and transport a specific substrate recognized at the outer leaflet of the membrane.

Another possibility is that the V shape observed in the crystal structure of NorM, which is polyspecific for hydrophobic drugs, may originate from the fact the extracellular vestibule is actually not empty in the crystal structure and that detergent molecules that have not been resolved in the crystal structure may be bound in the vestibule in a manner similar to what has been found for the nicotinic acetylcholine receptor.[30] Figure S2 of the Supporting Information provides a direct representation of the quality of the electron density map for the residues exposed to the outward-facing cavity. In the center of the cavity, it is possible to observe some weak electron density peaks corresponding to solvent atoms, but at the current resolution, it is not possible to identify what molecules may occupy those sites. It must also be considered that if detergent molecules would stabilize the inner face of the cavity in the solubilized form of NorM, they would not necessarily need to be ordered in the crystal, and consequently, they would not be visible in the electron density.

dx.doi.org/10.1021/bi2015184 | *Biochemistry* 2012, 51, 1281−1287

Sodium Ions Can Access the Binding Pocket via Binding to D36. Despite the fact that the large change in the extracellular vestibule observed in the MD simulations may suggest a transition of the transporter to a conformation that resembles that of the occluded state, it must be noted that the binding pocket formed by E255 and D371 remains constantly connected with the extracellular medium by a narrow permeation pathway. Interestingly, this novel permeation pathway that is obtained after the collapse of the extracellular vestibule involves D36, a residue that has been found to be crucial for transport activity in NorM from *Vibrio parahemolyticus*, a transporter of the MATE family that is 76% identical in sequence to that described in this study.[17] Close inspection of the crystal structure, on the other hand, does not show any obvious relation between this residue and the mechanism of ion transport, and no Rb^+ electron density was observed in the proximity of D36 in the X-ray structure.[9]

To study the binding of Na^+ ions to the transporter in its apo form, we started four additional MD runs from different initial conditions (MD runs f–i). In detail, MD runs f and g are started from the structure of MD runs d and e, respectively, after 10 ns of unrestrained MD, while MD runs h and i are initiated from MD runs d and e, respectively, after 100 ns of unrestrained MD. In all cases, 10 Na^+ ions (together with 10 Cl^- ions to keep the system neutral) are placed in the bulk solvent before the new simulations are started. Spontaneous binding of Na^+ is observed within hundreds of nanoseconds in three of the four independent MD simulations. The binding event invariably proceeds through binding of Na^+ to D36 (Figure 4), thus providing a possible rationale for why mutation

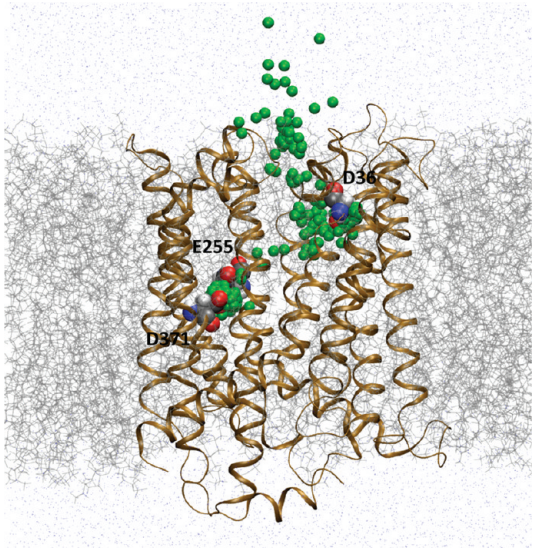

Figure 4. Spontaneous entry of a sodium ion into the binding site of NorM. Sodium (green) accesses the binding site formed by E255 and D371 via an intermediate step that implies binding of the cation to residue D36. The coordinates of the sodium ion (green) are taken from two independent MD simulations and are plotted at fixed time intervals vs a representative structure of the transporter from one of the two simulations.

of this residue inhibits protein function.[17] This transient interaction is characterized by a pentacoordinated structure (coordination number of 5.3), formed by the two side chain oxygens of D36, together with two water molecules with either one additional water molecule or a direct interaction with a surrounding residue (the most populated partners from the simulations are the backbone oxygen of residue M134 and the side chain oxygen of T200).

In addition, in one simulation (MD run f), a spontaneous rebinding of Na^+ to the binding site suggested by the crystallographic structure, formed by residues E255 and D371, is observed. The rapidity of this rebinding event, especially in comparison with the other simulations, is probably a consequence of the initial configuration, in which the extracellular lumen has not yet fully collapsed. However, it is noteworthy that even in this case the rebinding passes through D36, instead of directly proceeding toward E255 and D371.

Even though quantitative prediction of the binding free energy profile and, hence, of the binding affinity of Na^+ for the transporter in its various conformations would require the explicit computation of the potential of mean force (PMF) using enhanced sampling techniques,[31,32] which are outside the scope of this study, it is interesting to notice that, within the time scales of our simulations, once the sodium ion is bound to D36, it never spontaneously goes back toward the bulk, giving a qualitative indication that the barrier for the backward reaction is higher than the barrier for the forward one.

Finally, with respect to the substrate stoichiometry of NorM, which is not yet known experimentally, we report that during our simulations we have not obtained any evidence of a knock-on mechanism to drive the translocation of cations from D36 to the crystallographic binding site formed by E255 and D371, because we never observe the presence of more than one Na^+ inside the transmembrane bundle of the transporter.

Sodium Can Bind to the Dyad Formed by E255 and D371 in Two Distinct Modes. In addition, the MD simulations of the transporter bound to a Na^+ ion reveal the molecular details of the coordination environment of the cation inside the binding pocket. In the crystal structure, a Rb^+ ion is located in the proximity of catalytic residues E255 and D371 but does not interact directly with them. Instead, the closest residues to the Rb^+ ion are aromatic residues F259, F288, Y367, and F429. As a consequence, the coordination geometry of Rb^+ is extremely atypical of metal ions. On the other hand, MD simulations may offer an interesting alternative for studying the coordination of metal ions (and Na^+ in particular) inside the binding pocket of NorM.

Depending on the relative distance between residues E255 and D371, two clearly distinct binding modes are observed (Figure 5). In the first one, a competitive binding between E255 and D371 is established with spontaneous switching between the two conformations, as shown in the top and middle panels of Figure 5. In the second one, on the other hand, the two residues approach each other (the C_α–C_α distance between E255 and D371 decreases from 13.8 Å in the crystal structure to an average of 10.2 Å in this conformation, while the C_γ–C_γ distance between the two acidic residues is reduced from 8.5 to 4.5 Å) and are able to simultaneously bind the Na^+ ion (Figure 5, bottom panel).

In the competitive binding mode, the ion presents a pentacoordinated (coordination number of 5.4) structure composed by fast-switching water molecules and by the side chain oxygens of either E255 or D371 (Figure 5). In the second binding mode, where the sodium is simultaneously bound to E255 and D371, the coordination number of the ion is 5.6 and its ligand sphere is composed of the four side chain oxygens of E255 and D371 with one or two additional water molecules. For both binding modes, the MD simulations indicate that

dx.doi.org/10.1021/bi2015184 | *Biochemistry* 2012, 51, 1281–1287

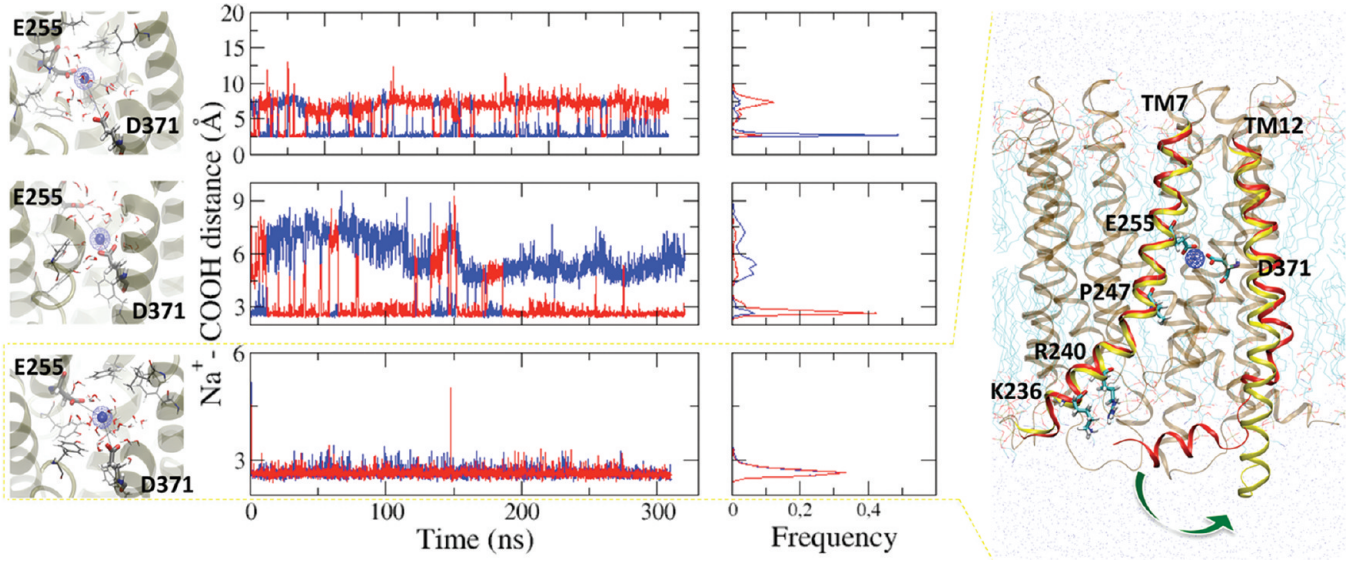

Figure 5. Molecular interactions of E255 and D371 with the bound sodium ion in three independent MD simulations (left). Time evolution of the distance between the Na^+ ion and the C_δ atom of E255 (blue) and the C_γ atom of D371 (red) in the binding pocket and corresponding histograms (middle). The MD simulations suggest two possible binding modes: a competitive binding mode (top and middle) and a simultaneous binding mode (bottom). Intracellular gating movement of the C-terminus of NorM upon simultaneous binding of sodium by E255 and D371 (right). The initial conformation of TM7 and TM12 is colored red, while the final one is colored yellow. E255 and D371 simultaneously binding the sodium ion are explicitly shown as licorice together with residues K236, R240, and P247 that are involved in the observed mechanism. The sodium ion is colored blue in solvent representation. The movement of TM12 allows permeation of the central cavity by water and thus, potentially, uptake of drug from the cytoplasm.

while aromatic residues remain close to the Na^+, they do not directly interact with the ion, as expected from the standard coordination geometry of metal ions in protein binding sites.

Finally, it is interesting to notice that in the latter binding mode, where the sodium is simultaneously bound to E255 and D371, a transition of the α-helical portion of the C-terminus that is not evolutionarily conserved across the family is observed. The helix is displaced from a conformation parallel to the membrane bilayer toward a perpendicular orientation (Figure 5, right panel). During this motion, the C-terminus becomes an extension of TM12 and water molecules can access the central cavity of the transporter from the cytoplasm. This movement is never observed in any of the simulations where the sodium ion is competitively bound by only one of the two acidic residues (or when it is in the apo form), including the ones in which Na^+ was initially placed in the Rb^+ binding site.

This movement is triggered by the disruption of some salt bridges between the C-terminus of TM12 and charged residues (K236 and R240) of the N-terminal part of TM7 [some of them are already present in the crystal (K236), while others form during the MD simulations (R240)]. The disruption of these interactions, which help keep the C-terminus of TM12 in the crystallographic conformation, is induced by a straightening of TM7 around the hinge formed by evolutionarily conserved[33] proline P247 as a consequence of E255 approaching D371 to achieve the simultaneous binding of the Na^+ ion (Figure 5 and Figure S9 of the Supporting Information). This movement opens the cytoplasmatic half of the protein to water permeation, because the C-terminus of TM12 acts as a lid, preventing the access of water to the intracellular moiety of the transporter. We speculate that this conformational change could be involved in the outward-facing to inward-facing transition, allowing for uptake of drug in the catalytic site from the cytoplasm.

CONCLUSIONS

In summary, equilibrium MD simulations of the multidrug and toxic compound extrusion (MATE) transporter NorM indicate that the large extracellular vestibule of the protein suggested by the crystallographic data is unstable under native conditions and is reduced to a narrow and twisting permeation pathway. The newly formed permeation pathway connects the external environment with the catalytic site through D36, and binding of the sodium ion to this residue is found to be a necessary intermediate for Na^+ binding to the cleft surrounding E255 and D371. Two distinct binding modes of the sodium ion inside the binding pocket of the transporter are observed: in the first, competition between E255 and D371 is established, with the ion binding alternatively to only one of the two acidic residues, and in the second, the Na^+ is simultaneously bound to E255 and D371, even though these two residues are quite far apart in the crystal structure. Once the cation is simultaneously bound to E255 and D371, a conformational change in the α-helical portion of the C-terminus, from an orientation parallel to the membrane bilayer to a perpendicular direction, takes place. This transition may be a precursor of a larger conformational change that leads the transporter toward the inward-facing conformation, allowing for potential uptake of drug from the intracellular environment. Finally, the observation that the V shape suggested by the X-ray data is invariably reduced to a narrow permeation pathway, together with the available crystal structures of evolutionarily related transporters of the MFS, might suggest that differences in the hydrophobic content of the extracellular vestibule may characterize multidrug resistance transporters (NorM and EmrD) in contrast with more substrate-selective members of the MFS (FucP, LacY, and GlpT). In particular, a wide V-shaped extracellular vestibule may not be a structural requisite in the substrate-free outward-facing conformation of multidrug secondary active transporters,

dx.doi.org/10.1021/bi2015184 | *Biochemistry* 2012, 51, 1281−1287

because these transporters do not have to recognize and bind a specific substrate at the outer leaflet of the membrane, where they need to selectively bind only cations to perform their catalytic cycle.

■ ASSOCIATED CONTENT

Supporting Information

One table and nine figures. This material is available free of charge via the Internet at http://pubs.acs.org.

■ AUTHOR INFORMATION

Corresponding Author

*E-mail: ursula.roethlisberger@epfl.ch. Telephone: +41-(0)21-693-0321. Fax: +41-(0)21-693-0320.

Funding

This work was supported by Swiss National Science Foundation Grant 200020-116294.

■ REFERENCES

(1) Aller, S. G., Yu, J., Ward, A., Weng, Y., Chittaboina, S., Zhuo, R., Harrell, P. M., Trinh, Y. T., Zhang, Q., Urbatsch, I. L., and Chang, G. (2009) Structure of P-glycoprotein reveals a molecular basis for poly-specific drug binding. *Science 323*, 1718−1722.

(2) Murakami, S., Nakashima, R., Yamashita, E., and Yamaguchi, A. (2002) Crystal structure of bacterial multidrug efflux transporter AcrB. *Nature 419*, 587.

(3) Yin, Y., He, X., Szewczyk, P., Nguyen, T., and Chang, G. (2006) Structure of the multidrug transporter EmrD from *Escherichia coli*. *Science 312*, 741−744.

(4) Krishnamurthy, H., Piscitelli, C. L., and Gouaux, E. (2009) Unlocking the molecular secrets of sodium-coupled transporters. *Nature 459*, 347−355.

(5) Jardetzky, O. (1966) Simple allosteric model for membrane pumps. *Nature 211*, 969−970.

(6) Tanford, C. (1983) Translocation pathway in the catalysis of active transport. *Proc. Natl. Acad. Sci. U.S.A. 80*, 3701−3705.

(7) Kaback, H. R., Dunten, R., Frillingos, S., Venkatesan, P., Kwaw, I., Zhang, W., and Ermolova, N. (2006) Site-directed alkylation and the alternating access model for LacY. *Proc. Natl. Acad. Sci. U.S.A. 104*, 491−494.

(8) Forrest, L. R., Kramer, R., and Ziegler, C. (2011) The structural basis of secondary active transport mechanisms. *Biochim. Biophys. Acta 1807*, 167−188.

(9) He, X., Szewczyk, P., Karyakin, A., Evin, M., Hong, W. X., Zhang, Q., and Chang, G. (2010) Structure of a cation-bound multidrug and toxic compound extrusion transporter. *Nature 467*, 991−994.

(10) Omote, H., Hiasa, M., Matsumoto, T., Otsuka, C., and Moriyama, Y. (2006) The MATE proteins as fundamental transporters of metabolic and xenobiotic organic cations. *Trends Pharmacol. Sci. 27*, 587−593.

(11) Van Veen, H. W. (2010) Last of the multidrug transporters. *Nature 467*, 926−927.

(12) Dang, S., Sun, L., Huang, Y., Lu, F., Liu, Y., Gong, H., Wang, J., and Yan, N. (2010) Structure of a fucose transporter in an outward-open conformation. *Nature 467*, 734−738.

(13) Newstead, S., Drew, D., Cameron, A. D., Postis, V. L. G., Xia, X., Fowler, P. W., Ingram, J. C., Carpenter, E. P., Sansom, M. S. P., McPherson, M. J., Baldwin, S. A., and Iwata, S. (2011) Crystal structure of a prokaryotic homologue of the mammalian oligopeptide-proton symporters, PepT1 and PepT2. *EMBO J. 30*, 417−426.

(14) Paulsen, I. T., Brown, M. H., and Skurray, R. A. (1996) Proton-dependent multidrug efflux systems. *Microbiol. Rev. 60*, 575.

(15) Abramson, J., Smirnova, I., Kasho, V., Verner, G., Kaback, H. R., and Iwata, S. (2003) Structure and mechanism of the lactose permease of *Escherichia coli*. *Science 301*, 610−615.

(16) Pao, S. S., Paulsen, I. T., and Saier, M. H. (1998) Major facilitator superfamily. *Microbiol. Mol. Biol. Rev. 62*, 1−34.

(17) Otsuka, M., Yasuda, M., Morita, Y., Otsuka, C., Tsuchiya, T., Omote, H., and Moriyama, Y. (2005) Identification of essential amino acid residues of the NorM Na^+/Multidrug Antiporter in *Vibrio parahaemolyticus*. *J. Bacteriol. 187*, 1552−1558.

(18) Wolf, M. G., Hoefling, M., Aponte-Santamaria, C., Grubmuller, H., and Groenhof, G. (2010) g_membed: Efficient insertion of a membrane protein into an equilibrated lipid bilayer with minimal perturbation. *J. Comput. Chem. 31*, 2169−2174.

(19) Van der Spoel, D., Lindahl, E., Hess, B., Groenhof, G., Mark, A. E., and Berendsen, H. J. C. (2005) GROMACS: Fast, Flexible and Free. *J. Comput. Chem. 26*, 1701−1718.

(20) Klauda, J. B., Venable, R. M., Freites, A., O'Connor, J. W., Tobias, D. J., Mondragon-Ramirez, C., Vorobyov, I., Mackerell, A. D., and Pastor, R. W. (2010) Update of the CHARMM all-atom additive force field for lipids: Validation on six lipid types. *J. Phys. Chem. B 114*, 7830−7843.

(21) Bjelkmar, P., Larsson, P., Cuendet, M. A., Bess, B., and Lindhal, E. (2010) Implementation of the CHARMM force field in GROMACS: Analysis of protein stability effect from correction maps, virtual site and water models. *J. Chem. Theory Comput. 6*, 459−466.

(22) Jorgensen, W. L., Chandrasekhar, J., Madura, J. D., Impey, R. W., and Klein, M. L. (1983) Comparison of simle potential functions for simulating liquid water. *J. Chem. Phys. 79*, 926−935.

(23) Essmann, U., Perera, L., Berkowitz, M. L., Darden, T., Lee, H., and Pedersen, L. G. (1995) A smooth particle mesh Ewald method. *J. Chem. Phys. 103*, 8577−8593.

(24) Hess, B., Bekker, H., Berendsen, H. J. C., and Fraaije, J. G. E. M. (1997) LINCS: A linear constraint solver for molecular simulations. *J. Comput. Chem. 18*, 1463−1472.

(25) Berendsen, H. J. C., Postma, J. P. M., Vangunsteren, W. F., and Hermans, J. (1981) Interaction models for water in relation to protein hydration. *Intermol. Forces,*, 331−342.

(26) Berendsen, H. J. C., Postma, J. P. M., Vangunsteren, W. F., Dinola, A., and Haak, J. R. (1984) Molecular-dynamics with coupling to an external bath. *J. Chem. Phys. 81*, 3684−3690.

(27) Humphrey, W., Dalke, A., and Schulten, K. (1996) VMD: Visual Molecular Dynamics. *J. Mol. Graphics 14*, 33−38.

(28) The PyMOL Molecular Graphics System, Version 1.4.1, Schrödinger, LLC.

(29) Huang, Y., Lemieux, M. J., Song, J., Auer, M., and Wang, D. N. (2003) Structure and mechanism of the glycerol-3-phosphate transporter from *Escherichia coli*. *Science 301*, 616−620.

(30) Brannigan, G., Henin, J., Law, R., Eckenhoff, R., and Klein, M. L. (2008) Embedded cholesterol in the nicotinic acetylcholine receptor. *Proc. Natl. Acad. Sci. U.S.A. 105*, 14418−14423.

(31) Allen, T. W., Andersen, O. S., and Roux, B. (2006) Molecular dynamics: Potential of mean force calculations as a tool for understanding ion permeation and selectivity in narrow channels. *Biophys. Chem. 124*, 251−267.

(32) Deng, Y., and Roux, B. (2009) Computations of standard binding free energies with molecular dynamics simulations. *J. Phys. Chem. B 113*, 2234−2246.

(33) Singh, A. K., Haldar, R., Mandal, D., and Kundu, M. (2006) Analysis of the topology of *Vibrio cholerae* NorM and identification of amino acid residues involved in norfloxacin resistance. *Antimicrob. Agents Chemother. 50*, 3717−3723.

(34) Smart, O. S., Neduvelil, J. G., Wang, X., Wallace, B. A., and Sansom, M. S. (1996) HOLE: A program for the analysis of the pore dimensions of ion channel structural models. *J. Mol. Graphics 14*, 354−360, 376.